Geomechanics and Engineering, *Vol. 25, No. 3 (2021) 171-178*
DOI: https://doi.org/10.12989/gae.2021.25.3.171

Wave-structure interaction of coastal reinforced concrete piles with bracing and different arrangements

Mohammad Rezazadeh Ghorbanipour[1a] and Hamed Sarkardeh*[2]

[1]*Department of Civil Engineering, Alaodoleh Semnani University of Higher Education, Garmsar, Iran*
[2]*Department of Civil Engineering, Faculty of Engineering, Hakim Sabzevari University, Sabzevar, Iran*

(Received July 2, 2019, Revised November 18, 2020, Accepted April 4, 2021)

Abstract. Wave interaction in marine structures is an important issue where requires to be considered in view of number of bases, piles and arrangement method. In this research, effect of waves and their forces on piles with different arrangements was investigated using numerical modeling. Simulations were performed in presence of bracing elements between piles against the force of waves and also were compared with simple arrangement without bracing elements in different arrangements. Results showed that in models that were fitted with bracing elements, the displacement rate reduced about 96%, and tension tolerances increased more than 53% and abutment responses also decreased about 70%.

Keywords: ocean waves; structural reaction; pile bracing; numerical modeling; pile arrangement

1. Introduction

Piles and decks are of the most used coastal structures and ports, which connect the structure to the ground under the sea. Considering the size of the marine structures and expected load bearing capacity, a number of piles with different diameters and alignments are needed. In the beach area, piles play an obstacle rule in the waves path and they can be affected by waves and undergo structural changes according to the arrangement. There are two classical theories to express the behavior of simple waves, Airy theory that was introduced in 1845 and Stokes theory which was expressed in 1880. Airy and Stokes theories generally predicted the waves behavior of those the water depths and their wavelengths ratio are not very small. Generally, Fig. 1 can be used to select the most appropriate wave theory according to the water depth and wave characteristics.

Regarding Fig. 1, Stokes theory is used in the current study. One of the conditions of this theory is that (H/d) ratio be so small that the theory can only be applied in deep water and part of the moderate waters range. Depends on the type and dimensions of used members in an offshore structure that determines the type of wave-structure interaction regime, one of the methods: Morison equation, Froude-Krylov theory, Diffractio theory can be used to calculate the wave force. In this research, the Morison equation is used due to the type simulation. Morison equation expresses the force applied to the length unit of the member, is defined as the Eq. (1):

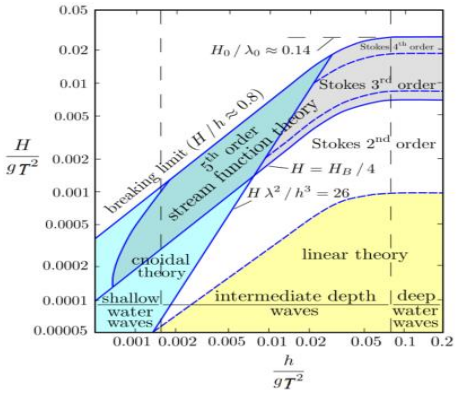

Fig. 1 Wave profile based on LeMehaute's 1969 work

$$f = C_I A_I \frac{\partial u}{\partial t} + C_D A_D |u|u \tag{1}$$

That values A_D and A_I are the form of Eq. (2):

$$A_I = \rho \frac{\pi}{4} D^2 \quad , \quad A_D = \frac{1}{2}\rho D \tag{2}$$

where, $\partial u/\partial t$ is the particle local horizontal acceleration (local acceleration), u is the particle horizontal velocity, ρ is the water specific mass, D is the base diameter and C_D is the drag coefficient and C_I is a function of the particles horizontal velocity and existing period. Two hydrodynamic non-dimensional parameters of Reynolds number (Re) and the Keulegan-Carpenter number (KC) in Eq. (3) are used to illustrate effects of factors such as particle velocity, existing period, base diameter and fluid viscosity:

$$R_e = \frac{u_{max} D\rho}{\mu} \quad , \quad KC = \frac{u_{max} T}{D} \tag{3}$$

∗Corresponding author, Associate Professor
E-mail: sarkardeh@hsu.ac.ir
[a]M.Sc. Student
E-mail: mohammad17rezazadeh@gmail.com

ISSN: 2005-307X (Print), 2092-6219 (Online)

where, u_{max} is the particles maximum horizontal velocity, T is the wave period and μ is the dynamic viscosity. It should be noted that C_D and C_I values determines by experiment. The range of these coefficients according to the American Petroleum Institute (API) regulations (API 2000) is chosen in the range of 0.6 to 1.0 for the coefficient drag and 1.5 to 2.0 for the inertia coefficient, respectively. Layout and type selection of these structures will be of great help in design and implementation to correct operation with high performance and less damage to the structure and its longer life. Where it can be possible just by careful review and consideration of various parameters by precise methods such as numerical methods. Around the mentioned issues, some studies have taken place in recent years in the world.

In order to examine the designed hydraulic structures in different conditions and optimize the design parameters, using physical models and laboratory tests is a common idea (Sarkardeh *et al.* 2010, Solaimani *et al.* 2017, Hosseini *et al.* 2017). Truitt and Herbich (1986) experimentally evaluated the transmission of random waves through pile breakwaters and found that there is little difference in the calculated transmission coefficients simultaneously the same parameters are used for both incident and transmitted spectra. Their results show that the transmission coefficient influences by water depth to wave height ratio (d/H). In spite of that, the impress of the breakwater geometry, i.e., the ratio of spacing to diameter (b/D) is more conspicuous.

Myrhaug and Rue (2005) investigated the Scour around group of slender vertical piles in random waves. They combined with describing the waves as a stationary Gaussian narrow-band random process to derive the scour depths in random waves. Zhao *et al.* (2013) studied three dimensional (3D) numerical model for wave-induced seabed response around breakwater heads. They found that the wave-induced pore pressures at breakwater heads are greater than that beneath a breakwater. Zhang *et al.* (2014) investigated the Large-scale pilot test study on bearing capacity of sea-crossing bridge main pier pile foundations. Results showed that the design is feasible and effective. This method can directly test bearing capacity of main pier pile foundations, and analysis bearing behaviors from test results of sensors which embedded in the pile. Koraim *et al.* (2014) investigated the wave transmission, reflection, and energy dissipation of the double rows of vertical piles suspending horizontal steel C shaped bars experimentally and theoretically under normal regular waves. Comparison between experiments and predictions showed that theoretical model provides a good estimate to the different hydrodynamic coefficients. Goel (2010) evaluated the approximate seismic displacement capacity of piles in marine oil terminals. Results showed that the simplified procedure is intended to be used for preliminary design of piles or as a check on the results from the detailed nonlinear static pushover analysis procedure, with material strain control, specified in the MOTEMS. Ko *et al.* (2011) also presented their results of simulations with Flow 3D software on internal wave generation and achieved reasonable data. Liu *et al.* (2011) investigated the numerical effects of interactions between individual waves and pile foreshore wave by Finite Volume Method (FVM) based on the Bhatnagar-Gross-Krook (BGK) model, and both numerical and experimental results showed that transmission coefficients and wave reflection are very sensitive to variation in wave height. El-Gamal *et al.* (2014) studied the Tethers tension force effect in the response of a squared tension leg platform subjected to ocean waves. They found that for short wave periods, the surge response consisted of small amplitude oscillations about a displaced position that is significantly dependent on tether tension force, wave height; whereas for longer wave periods, the surge response showed high amplitude oscillations that is significantly dependent on wave height, and that special attention should be given to tethers fatigue because of their high tensile static and dynamic stress. Moghaddam *et al.* (2015) performed an investigation on offshore pipeline laid on 3D seabed configuration by ABAQUS software. The general algorithm for the finite element approach is introduced. Feng *et al.* (2017) examined the lateral loading of a long base sea craft, with inclined columns by the aim of ANSYS software. Based on the results of this study, the vertical column tip displacement in permitted working conditions, approximately fitted with the horizontal force, linearly, as well as the single column- displacement formula and the long column craft-displacement formula were provided. They also compared their results of simulations and berth tests with theoretical formula and found results of simulations to be reasonably accurate. Zhang *et al.* (2017) examined the responses from the wave of the sea bed around a candle base marine platform. They presented that the dimensionless spacing of the piles has significant effects on wave propagation. The effect of waves shadow on variety of model piles decreases by increasing the dimensionless spacing of a pile. On the other hand, the characteristics of the model piles under the wave load compared in three kinds of time. Results showed some differences due to the phase difference between the pile and the shadow effect. Nagi *et al.* (2017) reviewed waves pulse events on a Tension Leg Platform (TLP) model, empirically. Simultaneous measurement tests about the wave height, rigid body movement, tension, and pressure distribution were also designed on the underside of the model deck. Their results showed a variety of measurements, as well as insights from deck-wave loads on platform behavior, foundation tensions, and provisional pressure. Kumar *et al.* (2017) studied the structural damage detection through longitudinal wave propagation using spectral finite element method. This paper investigated the damage identification of the concrete pile element through axial wave propagation technique using computational and experimental studies. The feasibility of the axial wave propagation technique is studied through the numerical simulations using Elementary rod theory and higher order love rod theory under Smoothed Finite Element Method (SFEM). Taylan (2016) examined the nearby pile protected space behavior, for offshore wind power converters. Results indicated that the piles in the side tension loads are supposedly tolerates less than that side pressure loads. In addition, the condition of the piles is more important in side tension. In Abbasi *et al.* (2018) study, the passage of waves through pile groups with different arrangements is investigated using a 3D numerical model. By performing different numerical simulations, the effect of coastal pile arrangements on wave pattern was studied and was compared with existing experimental data, and an acceptable agreement was achieved. Yuan *et al.* (2018) investigated the hydraulic conductivity estimation by considering the existence of piles. Results indicated that the

error, in the case which determines the hydraulic conductivity based on Effective Medium Theory (EMT), is less than that determined in the automatic inversion case. Park and Nam (2018) investigated behavior of integral abutment bridge with partially protruded piles. Results of the analysis indicate that the Integrated and Pile-bent abutment with Mechanically (IPM) bridge, as any other Integral Abutment Bridge (IAB), is influenced to a large extent by temperature and time-dependent loads. When these loads are applied, the stress on a pile in the IPM bridge decreases as the displacement of the pile top increases, because the piles protrude from the ground surface and no soil reaction is generated on the protruded pile. Khanmohammadi and Fakharian (2018) investigated the evaluation of performance of piled-raft foundations on soft clay. Their results indicated that choosing the proper combination of length and spacing for piles can lead to acceptable differential and total settlements while a high percentage of total bearing capacity of piles can be mobilized, which is an efficient solution for the project. Chau and Jiang (2001) examined a 3D pollutant transport model for the Pearl River Estuary. Akbarian *et al.* (2018) investigated experimental and computational fluid dynamics based numerical simulation of using natural gas in a dual-fueled diesel engine. Ramezanzadeh *et al.* (2019) reviewed experimental and numerical analysis of a nanofluidic thermosyphon heat exchanger. Salih *et al.* (2019) researched thin and sharp edges bodies-fluid interaction simulation using cut-cell immersed boundary method. Kim and Kim (2019) investigated a numerical method to simulate detonative combustion of hydrogen-air mixture in a containment Tabeshpour *et al.* (2020) conducted a research on challenges in the calculation of critical buckling load of tubular members of jacket platforms in finite element modeling. Shen and Liu (2017) reviewed current effects on global motions of a floating platform in waves. Myrhaug and Fu (2017) examined scour below pipelines due to random waves alone and random waves plus currents on mild slopes. Results for random waves alone and random wave plus currents presented and discussed by varying the seabed slope and water depth. Baghban *et al.* (2019) investigated towards experimental and modeling of heat transfer performance in quadrangular cross-section channels.

With respect to the before researches, this research was defined numerically to see the effect of waves on structural reactions of marine pile reinforced concrete structures. Simulations were performed in presence of bracing elements between pier piles against the force of waves and also were compared with simple arrangement without bracing elements in different arrangements and alignments for improving performance of piles in different wave loads.

2. Methods and materials

In the present simulations, piles are modeled in two Wire and Solid parts where the Solid part was inside the soil and Wire part was inside the fluid and associated with the flow of the wave. ABAQUS Software was used for applying the wave load, which load can be applied just on Wire type of the elements in the AQUA Environment. Reinforcement are also made in Wire shape. All bars of

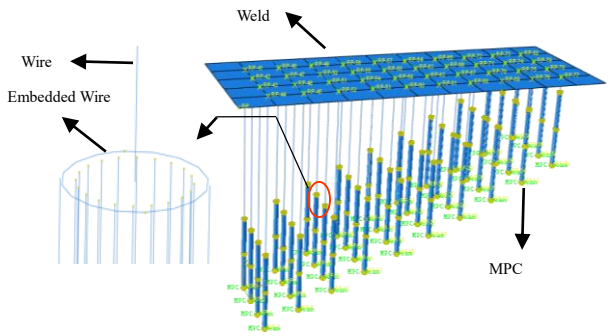

Fig. 2 Numerical simulated piles in the model

piles inside the concrete pile buried by embedding. The end of each pile with Multi Point Constraint (MPC) closure was bounded to a point on the central plate of the end of pile that this point will act as the representative of the whole plate of the piles. Head to each pile join to deck by Weld connector. Connectors are used also to connect bracing elements and head and tail of each bracing elements joined to the piles. Water is also not directly defined in terms of fluid and structure interaction, but also the wave load and fluid profile applied on ABAQUS Software. Water is also not directly defined in terms of fluid and structure interaction, but also the wave load and fluid profile applied on ABAQUS Software. Since the focus was on the structural discussion in this study and also a comparative discussion, adding soil-structure interaction only increased the analysis time and did not affect the desired results. Therefore, theory of fixed depth, which is also mentioned in the regulations, has been used (Fig. 2).

Two types of loads are defined for the model, which include weight wave loads. Weight load according to the regulations API considered as combination of dead weight and live weight and imported 5000 kilograms per square meter from the deck into piles. To apply wave load, AQUA in software is used. The type of wave is chosen from the regular non-linear stokes wave and solving wave equations by using Morison theory in AQUA. The basis of working with the environment AQUA is based on the fact that it is necessary to define its own fluid characteristics and the definition of the current and the wave as well as the wave loads, including the drag and inertia load for each element. Stokes type wave are applied with 5 meters high and zero degree radiation angle and period of 5 seconds for 3 alternating wave cycles in 15 seconds. Drag coefficient (C_D = 1) and inertia coefficient (C_M = 2) are considered, However, these coefficients are lower for the piles that are closer to the shore.

As mentioned in the first section, the range of drag and inertia coefficients is clear and decreases since the wave propagates towards the shore due to the effect of the shadow, so, the maximum values of coefficients of the farthest distance of piles from the beach is used in applying C_D and C_M. The applied wave load is also of the type of distributed loads. Since the sections of piles are circular, mesh type chosen Sweep. The mesh sizes considered 0.2 m in piles and 1 m in deck. Mesh convergence analysis are also used in numerical simulations to select the optimum

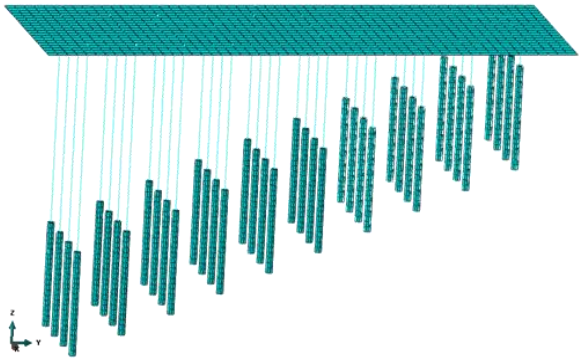

Fig. 3 Numerical simulated piles in the model

Table 1 Specifications of the simulated piles

Material	Reinforced Concrete
Number	40 numbers(4 row of 10)
Cross Section	Circular Section (d=70cm)
Rebar	20Φ250mm

Table 2 Different arrangements and layouts of piles

	Front view	Top view
A	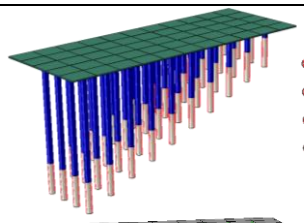	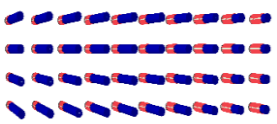
A-1	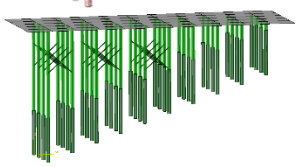	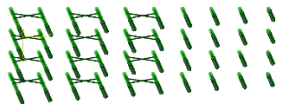
A-2	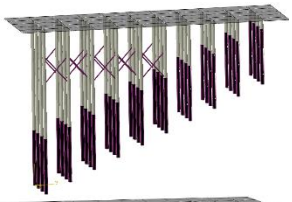	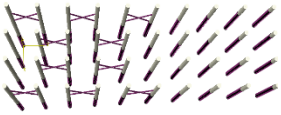
A-3	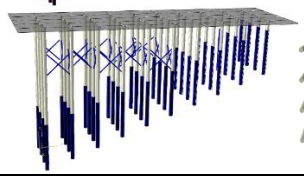	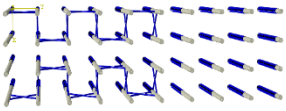

mesh size. The meshing and characteristics of the simulated piles are shown in Fig. 3 and Table 1.

At first, a scheme was modeled with direct piles and later added structural elements in different layouts and the effect of their existence is examined by comparing the amount of stresses and displacements. After constructing the initial model, a series of elements are considered by cross braces shape with a tube section made by steel. Then, it was modeled in three separate schemes with different layouts between the piles that are separately shown in Table 2 from two different views. These tubular shapes have a thickness of 10 mm and a diameter of 20 cm. The specifications of materials used in this study are presented

Table 3 Materials specifications

Materials	Parameter	Value
Concrete	Mass Density (kg/m^3)	2630
	Young Module (GPa)	30
	Poissons Ratio	0.2
Steel	Mass Density (kg/m^3)	7850
	Young Module (GPa)	2.1E11
	Poissons Ratio	0.3

Table 4 Tensile hardening and concrete tensile failure data

Displacement (mm)	Damage Parameter	Yield Stress (MPa)
0	0	2.90
0.066	0.381217	1.94
0.123	0.611070	1.30
0.173	0.763072	0.87
0.220	0.853393	0.59
0.265	0.909282	0.39
0.308	0.943865	0.26
0.351	0.965265	0.18
0.394	0.978506	0.12
0.438	0.986700	0.08
0.482	0.991770	0.05

Table 5 Specifications of the steel plastic

Yield Stress (Pa)	Plastic Strain
240754286	0
261512063	0.0045500
282960790	0.0091713
305870281	0.0179221
331191532	0.0327988
360055985	0.0555994
393775651	0.0878022
433843429	0.1304465
481933468	0.1840466
509559656	0.2149633
524375123	0.2314318

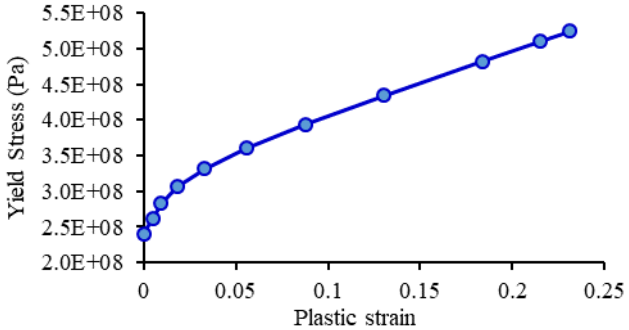

Fig. 4 Specifications of the steel plastic

also in Table 3. It should be noted that only reinforcement elements are used to apply wave load in two different types of arrangements in Figures A-1 and A-2, which are 12 and 10 in the A-1 and A-2 models, respectively. Also, model A-3 is simulated and examined by adding 10 reinforcement elements in the direction perpendicular to the wave load with the same arrangement of model A-2. Issues like the passage of installation channels that pass under the surface of the pier deck and also the ease of access to them for future repairs are also important in choosing the location of bracing elements. Therefore, different layout modes with specific conditions of each project can be selected with the most optimal mode.

It should be noted that nonlinear and linear behaviors of materials is considered in analysis. Since, nonlinear behavior of the structure hardness changes by its deformation. The tensile hardening data of the concrete tensile failure variables are presented in Table 4 and the specifications of the steel plastic in Table 5 and Fig. 4.

3. Results and discussions

Results of the present research were analyzed in three different categories of displacement, tension, and abutment reaction. The modeled flow characteristics are provided in Table 6. Simulated wave is executed according to the flow profile with the specifications mentioned in Table 6.

Table 6 Flow characteristics

Wave height	3 m
Wave period	5 s
Number of cycles on wave collision	15 s (For three intermittent wave cycles)
Direction of wave irradiance	Zero-degree angle
Flow rate	2 m/s

Table 7 Displacements

Model	Maximum Displacement (mm)
A	322
A-1	12
A-2	12
A-3	10

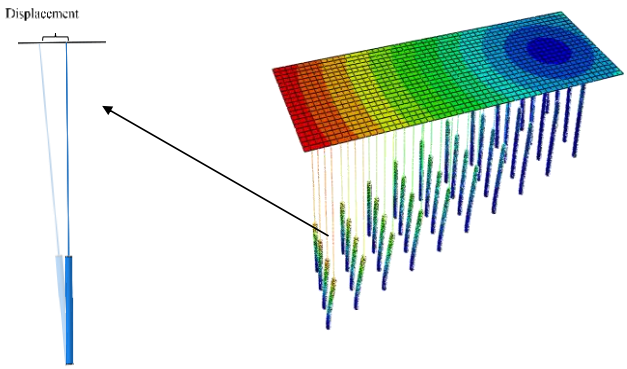

Fig. 5 Displacements of model A

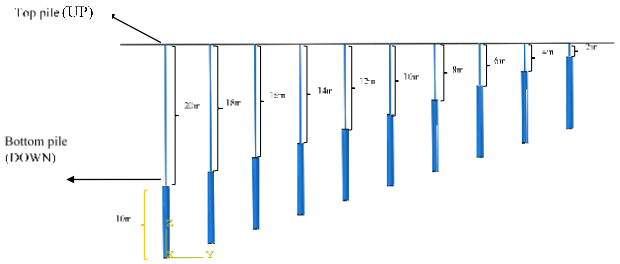

Fig. 6 Highest and lowest positions of piles

Table 8 Tension percentages for top and bottom of the piles

Element name	Top of the pile			Bottom of the pile		
	UP			DOWN		
	A-1	A-2	A-3	A-1	A-2	A-3
20 m	15.94	18.34	19.25	8.01	6.92	5.4
18 m	50.38	51.16	3.82	13.68	11.99	10.62
16 m	20.79	21.71	-0.14	13.57	12.53	6.59
14 m	35.5	37.97	2.42	17.13	15.79	7.69
12 m	26.08	25.96	0.38	16.29	16.48	8.4
10 m	23.7	24.17	1.29	-1.59	-1.19	6.54
8 m	-18.47	-10.25	-3.15	9.93	8.58	7.41
6 m	-16.75	-9.68	1.73	7.52	6.46	5.54
4 m	-16.41	-11.21	1.37	8.58	7.84	6.17
2 m	-12.97	-9.9	-6.18	7.93	8	5.09

3.1 Maximum displacement

In this section, results of displacement of the models according to the flow characteristics are given in Table 7 and shown in Fig. 5 for model (A) and displacement values for all models.

Deck displacement values: maximum displacement is about 0.32 m in the first model and is about 0.012 m in the second and third models. The layout of the second and third models is effective in reducing the displacement rate close to nearly 96% compared to the first model and the presence of bracing elements is able to significantly reduce the displacement (Table 7).

3.2 Comparison between tensions at the top and bottom of piles

In Table 8, the values of tensions are extracted once for the highest points of the piles and once for the lowest part that the results of each separately titled as UP and DOWN for the upper and lower points (Fig. 6).

Tensions at the top and bottom of the piles at different pile heights are shown in Figs. 7 and 8.

Concerning the top tensile of the pile, the results determine that (Fig. 7) exactly, at the part of embedded bracing elements (piles of 8 m to 20 m) reduction of tensions in different layouts between 19% and 51% can be resulted where for piles of 8 to 20 m, which bracing elements are not embedded, show a tensile increment of 6% to 18% (Table 8). In the case of bottom tensile strength of

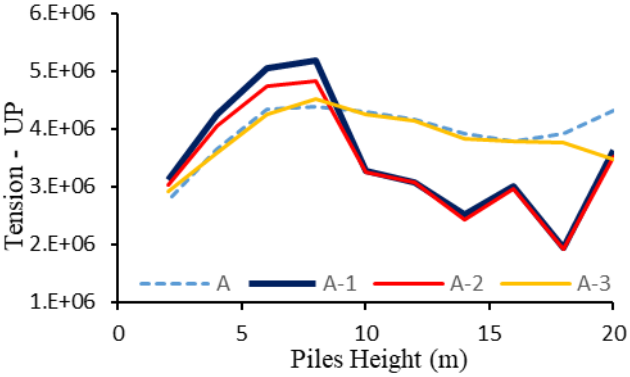

Fig. 7 Tensions at the top of the piles

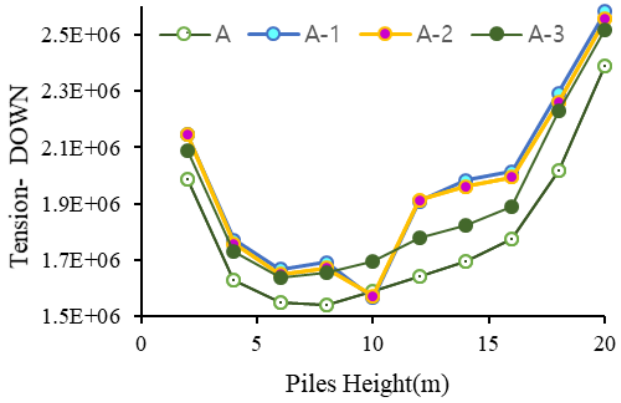

Fig. 8 Tensions at the bottom of piles

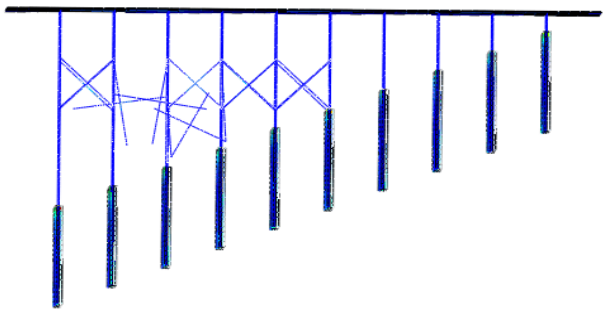

Fig. 9 Destruction of the braced elements

the piles (Fig. 8) results indicate that by placing the braced elements, tensile forms at the bottom of piles in the total structure increase by 10% to about 18%. The degree of tension was changed in models A-1 and A-2 due to destruction of the braced elements in that section (Fig. 9).

As shown in this figure, the reinforcement elements that are perpendicular to the wave, are destroyed. Therefore, the cross-sectional area, materials, arrangements and their angles should be further examined for each specific project.

3.3 Abutment reaction comparison

In this section, the reaction force of the candles is investigated. In such a way, the reaction force amount at the end of each pile in accordance with the derived force from the flow is extracted in Fig. 10 and compared in Table 9.

As shown in Fig. 10, when the abutment reactions in

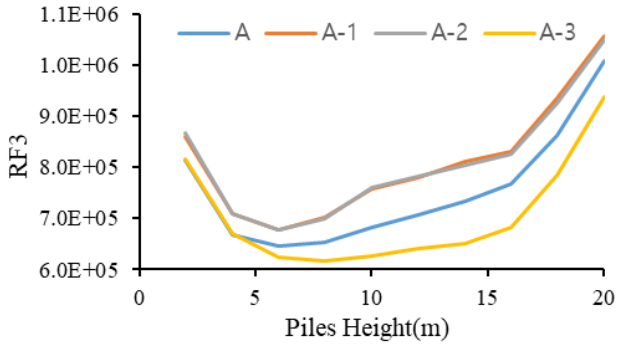

Fig. 10 Amount of abutment responses in the Z direction

Table 9 Reduction percentage of abutment responses in Z direction versus the first model

Element name	A-1	A-2	A-3
	RF3%	RF3%	RF3%
20 m	-4.92	-4.14	6.97
18 m	-8.44	-7.27	9.15
16 m	-8.34	-7.8	10.81
14 m	-10.59	-9.66	10.99
12 m	-10.22	-10.49	9.29
10 m	-11.1	-11.44	8.23
8 m	-7.67	-7.12	5.59
6 m	-5.25	-5.08	3.16
4 m	-6.14	-6.18	-0.04
2 m	-5.87	-6.62	-0.37

different models are compared together (Z direction), it can be seen a significant reduction in abutment response by placing the bracing elements. Thus, abutment reactions in the first model decreases about 18% close to 73% and in the second model, about 10% to more than 70% in third model and close to 11% in fourth model are obvious (Table 9).

4. Conclusions

The results showed that presence of bracing elements have a positive effect on increasing the resistance of the piles, although the kind of layout of those elements has also been effective in their impact. It can be concluded that in examining the amount of displacement on the deck, the layout of the fourth model could reduce the displacement up to 63%. The stress tolerance improved up to about 50% in the second and third model by embedding the bracing elements. Additionally, the abutment response in Z direction decreased up to 73% in the second model and by more than 70% in the third model. In the same way, results can be used for different arrangements of piles, including square or triangular cross-sections, changing different flow parameters such as wave angle, wavelength and periodicity. On the other hand, this numerical simulation method can be used for the decks that have already been implemented by adding reinforcement elements to examine their performance. Bracing elements between the piles to

strengthen the old decks can be a good solution that can be examined with this numerical method. Results of such as this studies can lead to construct piers with smaller sections.

Acknowledgments

The author would like to thank Dr. Mohammad Hadi Erfani for his helpful advice on various technical issues examined in this Paper.

References

Abbasi, A, Taghvaei, S.M. and Sarkardeh, H. (2018), "Numerical study on effect of coastal pile arrangements on wave characteristics", *J. Mar. Sci. Appl.*, **17**(4), 510-518. https://doi.org/10.1007/s11804-018-0039-z.

Abdussamie, N., Drobyshevski, Y., Ojeda, R., Thomas, G. and Amin, W. (2017), "Experimental investigation of wave-in-deck impact events on a TLP model", *Ocean Eng.*, **142**, 541-562. https://doi.org/10.1016/j.oceaneng.2017.07.037.

Akbarian, E., Najafi, B., Jafari, M., Faizollahzadeh Ardabili, S., Shamshirband, S. and Chau, K.W. (2018), "Experimental and CFD-based numerical simulation of using natural gas in a dual-fuelled diesel engine", *Eng. Appl. Comput. Fluid Mech.*, **12**(1), 517-534. https://doi.org/10.1080/19942060.2018.1472670.

Akdag, C.T. (2016), "Behavior of closely spaced double-pile-supported jacket foundations for offshore wind energy converters", *Appl. Ocean Res.*, **58**, 164-177. https://doi.org/10.1016/j.apor.2016.04.008.

API RP 2A WSD (2000), Recommended Practice for Planning, Designing and Constructing Fixed Offshore Platforms-Working Stress Design.

Baghban, A.R., Sasanipour, J., Pourfayaz, F., Ahmadi, M.H., Kasaeian, A., Chamkha, A., Oztop, H.F. and Chau, K.W. (2019), "Towards experimental and modeling study of heat transfer performance of water- SiO2 nanofluid in quadrangular cross-section channels", *Eng. Appl. Comput. Fluid Mech.*, **13**(1), 453-469. https://doi.org/10.1080/19942060.2019.1599428.

Chau, K.W. and Jiang, Y.W. (2001), "Three-dimensional pollutant transport model for the Pearl River estuary", *Water Res.*, **36**(8), 2029-2039. https://doi.org/10.1016/S0043-1354(01)00400-6.

El-Gamal, A.R., Essa, A. and Ismail, A. (2014), "Tethers tension force effect in the response of a squared tension leg platform subjected to ocean waves", *Ocean Syst. Eng.*, **4**(4), 327-342. https://doi.org/10.12989/ose.2014.4.4.327.

Goel, R.K. (2010), "Approximate seismic displacement capacity of piles in marine oil terminals", *Earthq. Struct.*, **1**(1), 129-146. https://doi.org/10.12989/eas.2010.1.1.129.

Hosseini, R., Fazloula, R., Saneie, M. and Amini, A. (2017), "Bagged neural network for estimating scour depth around pile groups", *Int. J. River Basin Manag.*, **16**(4), 401-412. https://doi.org/10.1080/15715124.2017.1372449.

Khanmohammadi, M. and Fakharian, K. (2018), "Evaluation of performance of piled-raft foundations on soft clay: A case study", *Geomech. Eng.*, **14**(1), 43-50. https://doi.org/10.12989/gae.2018.14.1.043.

Kim, D. and Kim, J. (2019), "Numerical method to simulate detonative combustion of hydrogen-air mixture in a containment", *Eng. Appl. Comput. Fluid Mech.*, **13**(1), 938-953. https://doi.org/10.1080/19942060.2019.1660219.

Ko, K.O., Choi, J.W., Yoon, S.B. and Park, C.B. (2011), "Internal wave generation in flow 3D model", *Proceedings of the 21st International Offshore and Polar Engineering Conference*, Maui, Hawaii, U.S.A., June.

Koraim, A.S., Iskander, M.M. and Elsayed, W.R. (2014), "Hydrodynamic performance of double rows of piles suspending horizontal c shaped bars", *Coast. Eng.*, **84**, 81-96. https://doi.org/10.1016/j.coastaleng.2013.11.006.

Kumar, K.V., Saravanan, T.J., Sreekala, R., Gopalakrishnan, N. and Mini, K.M. (2017), "Structural damage detection through longitudinal wave propagation using spectral finite element method", *Geomech. Eng.*, **12**(1), 161-183. https://doi.org/10.12989/gae.2017.12.1.161.

Liu, H., Ghidaoui, M.S., Huang, Z., Yuan, Z. and Wang, J. (2011), "Numerical investigation of the interactions between solitary waves and pile breakwaters using BGK-based methods", *Comput. Math. Appl.*, **61**(12), 3668-3677. https://doi.org/10.1016/j.camwa.2010.06.012.

Myrhaug, D. and Fu, P. (2017), "Scour below pipelines due to random waves alone and random waves plus currents on mild slopes", *Ocean Syst. Eng.*, **7**(3), 275-298. https://doi.org/10.12989/ose.2017.7.3.275

Myrhaug, D. and Rue, H. (2005), "Scour around group of slender vertical piles in random waves", *Appl. Ocean Res.*, **27**(1), 56-63. https://doi.org/10.1016/j.apor.2005.06.001.

Park, M.C. and Nam, M.S. (2018), "Behavior of integral abutment bridge with partially protruded piles", *Geomech. Eng.*, **14**(6), 601-614. https://doi.org/10.12989/gae.2018.14.6.601.

Ramezanizadeh, M., Nazari, M.A., Ahmadiand, M.H. and Chau, K.W. (2019), "Experimental and numerical analysis of a nanofluidic thermosyphon heat exchanger", *Eng. Appl. Comput. Fluid Mech.*, **13**(1), 40-47. https://doi.org/10.1080/19942060.2018.1518272.

Salih, S.Q., Aldlemy, M.S., Rasani, M.R., Ariffin, A.K., Ya, T.M.Y.S.T., Al-Ansari, N., Yaseen, Z.M. and Chau, K.W. (2019), "Thin and sharp edges bodies-fluid interaction simulation using cut-cell immersed boundary method", *Eng. Appl. Comput. Fluid Mech.*, **13**(1), 860-877. https://doi.org/10.1080/19942060.2019.1652209.

Sarkardeh, H., Zarrati, A.R. and Roshan, R. (2010), "Effect of intake head wall and trash rack on vortices", *J. Hydraul. Res.*, **48**(1), 108-112. https://doi.org/10.1080/00221680903565952.

Shaghaghi Moghaddam, A., Mohammadnia, S. and Sagharichiha, M. (2015), "Analysis of offshore pipeline laid on 3D seabed configuration by ABAQUS", *Ocean Syst. Eng.*, **5**(1), 31-40. https://doi.org/10.12989/ose.2015.5.1.031.

Shen, M. and Liu, Y. (2017), "Current effects on global motions of a floating platform in waves", *Ocean Syst. Eng.*, **7**(2), 121-141. https://doi.org/10.12989/ose.2017.7.2.121.

Solaimani, N., Amini, A., Banejad, H. and Taherei Ghazvinei, P. (2017), "The effect of pile spacing and arrangement on bed formation and scour hole dimensions in pile groups", *Int. J. River Basin Manag.*, **15**(2), 219-225. https://doi.org/10.1080/15715124.2016.1274321.

Tabeshpour, M.R., Erfani, M.H. and Sayyaadi, H. (2020), "Challenges in calculation of critical buckling load of tubular members of jacket platforms in finite element modeling", *J. Mar. Sci. Technol.*, **25**(3), 866-886. https://doi.org/10.1007/s00773-019-00686-5.

Truitt, C.L. and Herbich, J.B. (1986), "Transmission of random waves through pile breakwaters", *Proceedings of the 20th International Conference on Coastal Engineering*, Taipei, Taiwan, November.

Yaofeng, X., Liu, C., Gao, S., Tang, J. and Chen, Y. (2017), "Lateral load bearing capacity of offshore high-piled wharf with batter piles", *Ocean Eng.*, **142**, 377-387. https://doi.org/10.1016/j.oceaneng.2017.07.001.

Yuan, Y., Xu, Y.S., Shen, J.S. and Wang, B.Z.F. (2018), "Hydraulic conductivity estimation by considering the existence of piles: A case study", *Geomech. Eng.*, **14**(5), 467-477. https://doi.org/10.12989/gae.2018.14.5.467.

Zhang, Q., Zhou, X.L., Wang, J.H. and Guo, J.J. (2017), "Wave-induced seabed response around an offshore pile foundation platform", *Ocean Eng*., **130**, 567-582. https://doi.org/10.1016/j.oceaneng.2016.12.016.

Zhang, X., Li, Q., Ma, Y., Zhang, X. and Yang, S. (2014), "Large-scale pilot test study on bearing capacity of sea-crossing bridge main pier pile foundations", *Geomech*. *Eng*., **7**(2), 201-212. http://doi.org/10.12989/gae.2014.7.2.201.

Zhao, H.Y., Jeng, D.S., Zhang, Y., Zhang, J.S., Zhang, H.J. and Zhang, C. (2013), "3D numerical model for wave-induced seabed response around breakwater heads", *Geomech*. *Eng*., **5**(6), 595-611. http://doi.org/10.12989/gae.2013.5.6.595.

JS